The EMBO Journal Vol.16 No.22 pp.6646–6658, 1997

The crystal structure of a phosphorylase kinase peptide substrate complex: kinase substrate recognition

E.D.Lowe, M.E.M.Noble, V.T.Skamnaki[1], N.G.Oikonomakos[1], D.J.Owen[2] and L.N.Johnson[3]

Laboratory of Molecular Biophysics and Oxford Centre for Molecular Sciences, University of Oxford, Rex Richards Building, South Parks Road, Oxford OX1 3QU, UK, [1]National Hellenic Research Foundation, Institute of Biological Research and Biotechnology, 48, Vas Constantinou Avenue, Athens 116 35, Greece and [2]MRC Laboratory of Molecular Biology, Hills Road, Cambridge CB2 2QH, UK

[3]Corresponding author
e-mail: Louise@biop.ox.ac.uk

The structure of a truncated form of the γ-subunit of phosphorylase kinase (PHKγ_t) has been solved in a ternary complex with a non-hydrolysable ATP analogue (adenylyl imidodiphosphate, AMPPNP) and a heptapeptide substrate related in sequence to both the natural substrate and to the optimal peptide substrate. Kinetic characterization of the phosphotransfer reaction confirms the peptide to be a good substrate, and the structure allows identification of key features responsible for its high affinity. Unexpectedly, the substrate peptide forms a short anti-parallel β-sheet with the kinase activation segment, the region which in other kinases plays an important role in regulation of enzyme activity. This anchoring of the main chain of the substrate peptide at a fixed distance from the γ-phosphate of ATP explains the selectivity of PHK for serine/threonine over tyrosine as a substrate. The catalytic core of PHK exists as a dimer in crystals of the ternary complex, and the relevance of this phenomenon to its *in vivo* recognition of dimeric glycogen phosphorylase b is considered.

Keywords: catalytic mechanism/dimerization/ phosphorylase kinase/reversible phosphorylation/ substrate recognition

Introduction

Phosphorylase kinase (PHK) is a key enzyme involved in the control of glycogen degradation. The enzyme integrates extracellular signals arising from hormone receptor interactions and from neuronal impulses mediated through calcium with those arising from intracellular events, to provide a tightly controlled kinase activity which regulates glycogen phosphorylase. PHK is one of the largest of the protein kinases and is composed of four types of subunit, with stoichiometry $(\alpha\beta\gamma\delta)_4$, and a total mol. wt of 1.3×10^6 Da. Activity is regulated by cyclic AMP-dependent protein kinase phosphorylation, autophosphorylation, allosteric effectors (e.g. ADP), metal ion concentration (Ca^{2+} and Mg^{2+}), proteolysis and pH (Pickett-Gies and Walsh, 1986). The α and β subunits are regulatory and are the targets for control by phosphorylation. The δ subunit is essentially identical to calmodulin and confers Ca^{2+} sensitivity. The 386 amino acid γ subunit is the catalytic subunit which comprises an N-terminal kinase domain (residues 1–298) and a regulatory calmodulin-binding domain (residues 299–386).

In muscle and liver, PHK catalyses the Ca^{2+}-dependent phosphorylation of inactive glycogen phosphorylase b (GPb) to active glycogen phosphorylase a (GPa). Although *in vivo* the only definite substrate for PHK is glycogen phosphorylase, *in vitro* the enzyme will also phosphorylate, with lower activity, glycogen synthase, troponin I, troponin T, PHK α and β subunits and several other proteins (Pickett-Gies and Walsh, 1986). The site phosphorylated in GPb is Ser14. Analysis of sequences surrounding this and other sites recognized has led to a consensus sequence of Arg/Lys-X-X-Ser-Val/Ile-Y for possible substrates, where X and Y are any amino acids (Pearson and Kemp, 1991). Activity is considerably increased if residue Y is arginine as in phosphorylase (Graves, 1983). In brain, there is a high activity ratio of PHK to phosphorylase, an observation which has led to suggestions of possible alternative functions for PHK in neuronal tissue. Neuronal-specific protein B-50 (GAP-43), neurogranin and the microtubule-associated protein tau have been shown to be targets for PHK (Paudel *et al.*, 1993; Paudel, 1997).

As a first step towards understanding the structure and function relationships for this complex enzyme, we have determined the crystal structure of the kinase domain (residues 1–298) of the catalytic γ-subunit of phosphorylase kinase (PHKγ_t) in complex with the non-hydrolysable substrate analogue adenylyl imidodiphosphate (AMPPNP) (Owen *et al.*, 1995a) at a resolution of 2.5 Å. Subsequent higher resolution data collection on an XRIICCD detector, described here, has allowed determination of the conformations of some regions of the protein which were undefined in the original structure. Attempts to co-crystallize with a peptide substrate [residues 9–18 of GPb, Lys(–5)-Arg(–4)-Lys(–3)-Gln(–2)-Ile(–1)-Ser*(0)-Val(+1)-Arg(+2)-Gly(+3)-Leu(+4)] were not successful [Ser*(0) indicates the phosphorylatable serine: residues N-terminal and C-terminal to this residue are numbered –1, –2 etc. and +1, +2 etc. respectively]. Peptide substrates exhibit K_m values that are ~50-fold higher than the corresponding K_m values for phosphorylase itself (Graves, 1983), suggesting that structural features of the phosphorylase molecule may play a role in recognition. Indeed only one out of the 29 serines in the 842 amino acid glycogen phosphorylase molecule is phosphorylated, although some other serines are surrounded by a consensus sequence motif.

In order to elaborate on protein kinase specificity, Songyang *et al.* (1996) studied primary sequence specificity using an oriented degenerate peptide library and

Table I. Peptides and kinetic characterization

Subsite number:	–3	–2	–1	0	1	2	3	Total[b]	k_{cat} (min^{-1})	K_m (mM)	k_{cat}/K_m (min^{-1} mM^{-1})
Natural substrate	Lys	Gln	Ile	Ser	Val	Arg	Gly				
(Preference[a]):	2.5	1.7	1.5		1.5[c]	2.0	1.5[c]	28.8	70	1.8	40
Cantley peptide	Arg	Met	Met	Ser	Phe	Phe	Leu				
(Preference[a]):	5.7	2.0	2.2		3.9	2.5	2.1	513.5			
MC-peptide	Arg	Gln	Met	Ser	Phe	Arg	Leu				
(Preference[a]):	5.7	1.7	2.2		3.9	2.0	2.1	349.2	400	0.4	1000

[a]Preferences are the reported relative abundances of the given residue at the specific subsite position in a degenerate library of peptides phosphorylated by PHK, according to Songyang *et al.* (1996).
[b]The total preference value is the product of the preferences for each of the subsites of the given peptide.
[c]Songyang *et al.* do not report the relative abundance values for residues with a relative abundance below 1.5. Residues of the natural substrate peptide falling into this category are indicated. In order to obtain a maximum expected overall preference for the natural substrate peptide, these residues are assigned a preference of 1.5 in this analysis.

identified a so-called optimal peptide substrate (sequence Lys-Arg-Met-Met-Ser*-Phe-Phe-Leu-Phe). On the basis of the crystal structure and crystal lattice contacts for the PHKγ_t structure, we designed a modified version of this peptide (the 'modified Cantley' or MC-peptide), with a sequence closer to that of glycogen phosphorylase. In order to fit the available space, the peptide was truncated to seven residues, the minimum length peptide that is recognized without significant loss of activity (Graves, 1983). The methionine in the –2 position was replaced by a glutamine and the phenylalanine in position +2 was replaced by arginine, a residue which is known to be important in phosphorylase specificity (Graves, 1983). We have also synthesized a peptide of the same length, with a sequence identical to the phosphorylated site of phosphorylase (the 'natural substrate', or NS-peptide), for which we have determined the kinetic parameters as a substrate for PHKγ_t. We report the crystal structure of the ternary complex of PHKγ_t co-crystallized with the MC-peptide (sequence Ac-Arg-Gln-Met-Ser*-Phe-Arg-Leu) and AMPPNP. The results allow identification of the specific interactions that determine substrate specificity and also demonstrate an unexpected dimerization in which the catalytic sites of the kinase are separated by only 14 Å.

Results

Kinetics

The Michaelis–Menten kinetic parameters for PHKγ_t with two different peptide substrates are summarized in Table I. Of the two peptides, the higher affinity, as deduced from the K_m, is displayed by the modified Cantley peptide (MC-peptide, K_m = 0.4 mM), compared with the natural substrate peptide (NS-peptide, K_m = 1.8 mM). The factor of 25 in relative catalytic efficiency (k_{cat}/K_m) is consistent with the anticipated preference calculated on the basis of the position by position preferences observed by Songyang *et al.* (1996) at the different peptide subsites, which suggests that the MC-peptide would be a better substrate by a factor of at least 12.1. As previously observed, peptide substrates were poorer substrates than glycogen phosphorylase, for which K_m = 8.9 μM and k_{cat} = 4000/min. The MC-peptide behaves as a competitive inhibitor with respect to GPb, with a K_i of 0.6 mM (data not shown).

Higher resolution binary complex

Crystals of the binary complex between PHKγ_t and AMPPNP diffracted to a resolution of 2.1 Å. This diffraction limit had been observed previously, although attempts to collect a complete dataset to this resolution had been hindered by radiation-induced crystal decay, even under cryo-crystallographic conditions. The XRIICCD detector on BL4 of the ESRF allowed 180° of data to be collected in a period of ~2 h, compared with a typical period of 7 h for an equivalent data collection on a detector system with a longer read out cycle, such as an imaging plate. Over the course of this faster data collection, crystal decay was not apparent. The higher overall resolution thus obtained allowed the refinement of a more accurate model, which in turn allowed the positioning of several loops, notably the loop connecting strand β3 with the C-helix, which had previously not been traceable. The resulting model is complete from residue 14 through to residue 291. Statistics of the refined 2.1 Å model are given in Table II.

Ternary complex

PHKγ_t was crystallized in complex with the non-hydrolysable ATP analogue AMPPNP and the MC-peptide in the presence of manganese, and the structure solved at a resolution of 2.6 Å by molecular replacement. The refined 2.1 Å structure of the binary complex was used as the initial search model. Electron density is visible for residues 14–292 of PHKγ_t, for the whole of the substrate peptide and for AMPPNP with two manganese ions. Figure 1A shows electron density defining the conformation of the peptide in the refined 2mF_o–DF_c map. Although crystals with the MC-peptide complex grew readily and reproducibly, no crystals of the equivalent complex with the NS-peptide were obtained despite extensive trials.

The overall fold of PHKγ_t in the ternary complex resembles that of the binary complex described previously (Owen *et al.*, 1995a). A smaller N-terminal domain (residues 14–107), formed principally from β-sheet, is connected to a larger C-terminal domain (residues 110–292), formed mainly from α-helix. The two domains are joined by a hinge region around residues Lys108 and Gly109. The nucleotide binds at the cleft between the two domains, sandwiched between the glycine-rich hairpin

Table II. Data collection and refinement

Complex Beamline	Binary complex BL4, ESRF	Ternary complex Super ESCA, Elletra	Ternary complex D2AM, ESRF
Space group	$P2_12_12_1$	$P3_221$	$P3_221$
Cell	a = 47.7 Å, b = 67.7 Å, c = 110.8 Å	$a = b$ = 64.1 Å, c = 144.4 Å	$a = b$ = 65.3 Å, c = 145.8 Å
Maximum resolution	2.1 Å	3.45 Å	2.6 Å
Observations	137 663	14 119	21 644
Unique reflections	20 569	6927	10 062
R_{merge}[a]	0.047	0.188	0.098
Completeness	95.5%	89.9%	86.3%
Highest shell	2.21–2.10 Å	3.72–3.45 Å	2.74–2.60 Å
R_{merge}[a]	0.36	0.37	0.36
Completeness	79.1%	87.5%	78.1%
Refinement:			
Non-hydrogen atoms	2243 protein, 31 AMPPNP, 2 Mn^{2+}, 153 water	2092 protein, 65 peptide 31 AMPPNP, 2 Mn^{2+}	2243 protein, 65 peptide, 31 AMPPNP, 2 Mn^{2+}, 88 water, 6 glycerol
R_{conv}[b]	19.8% (6.0–2.1 Å)	35.3% (25.0–3.5 Å)	23.6% (25.0–2.6 Å)
R_{free}[c]	28.8% (6.0–2.1 Å)	35.3% (25.0–3.5 Å)	30.0% (25.0–2.6 Å)
R.m.s.ds from ideal geometry:			
Bonds[d]	0.006 Å	0.014 Å	0.005 Å
Angles[d]	1.7°	1.5°	1.8°
Ramachandran plot[e]	89.6%	89.1%	90.4%

[a] $R_{merge} = \dfrac{\sum_h \sum_j I_{h,j} - \bar{I}_h}{\sum_h \sum_j I_{h,j}}$ where $I_{h,j}$ is the intensity of the jth observation of unique reflection h.

[b] $R_{conv} = \dfrac{\sum_h ||Fo_h| - |Fc_h||}{\sum_h |Fo_h|}$ where Fo_h and Fc_h are the observed and calculated structure factor amplitudes for reflection h.

[c] R_{free} is equivalent to R_{conv} for a randomly selected 5% subset of reflections not used in structure refinement.
[d] As calculated by REFMAC (Murshudov *et al.*, 1997).
[e] Residues in the most favoured regions of the Ramachandran plot as calculated by PROCHECK (Laskowski *et al.*, 1993).

formed by strands β1 and β2, and a surface from the C-terminal domain. The C-terminal domain contains the 'activation segment', a stretch of residues between the conserved DFG and APE protein kinase motifs (Hanks and Quinn, 1991) which contains the site of activatory phosphorylation of many protein kinases (but not PHK) that are controlled by phosphorylation of the catalytic domain (Johnson *et al.*, 1996).

The MC-peptide binds in the active site groove of PHKγ$_t$ (Figure 1B), following a path very similar to that of the equivalent residues of the protein kinase inhibitor PKI bound to cAPK. This similarity of binding breaks down, however, over the C-terminal two residues of the MC-peptide. Binding of the peptide is achieved through marked complementarity of shape, hydropathy and potential, as suggested from the GRASP image in Figure 1C.

Contacts of the substrate peptide to PHKγ$_t$

Polar contacts involving the MC-peptide in complex with PHKγ$_t$ are summarized in Figure 2A. Arg(–3) forms an ion pair with Glu110 from the hinge region, which interacts in turn with the O2′ and O3′ ribose oxygens of the nucleotide substrate. The involvement of this residue in binding basic residues at the P-3 site had been anticipated by site-directed mutagenesis (Huang *et al.*, 1995). The amide oxygen of Gln(–2) is hydrogen bonded with the main chain nitrogen of Ser188, and the amide nitrogen is close (3.75 Å) to the OG atom of the same residue. Ser188 is part of a single turn of α-helix close to the end of the activation segment. The peptide oxygen of Gln(–2) is 3.4 Å from the NZ atom of Lys151, and hydrogen bonded to a water. No hydrogen bonds are observed for Met(–1).

The OG atom of Ser(0), the nucleophile in the phosphotransfer reaction, is poised 3.6 Å from the phosphorus atom of the imidophosphate group of the nucleotide substrate analogue. The closest contact of the OG atom is a distance of 2.6 Å to an imidophosphate terminal oxygen.

The other polar side chain contact involves Arg(+2), which appears from the electron density to have some conformational variability. The best defined conformation for this side chain positions it to interact with the side chain of Glu182, the residue in PHK which plays an analogous role to the phosphorylated residues Thr197 (in cAPK) or Thr160 (in CDK2).

The most striking aspect of the polar interactions between the MC-peptide and PHKγ$_t$ is the existence of a short stretch of anti-parallel β-sheet formed by Phe(+1) and Leu(+3) peptide which hydrogen-bonds with Gly185 and Val183 from the enzyme. This interaction is consistent with the extended conformation of this end of the peptide substrate, and of these residues from the protein. The mutation of the residue corresponding to Gly185 to Glu in the testis/liver isoform of phosphorylase kinase causes autosomal liver glycogenosis (Maichele *et al.*, 1996). The structure suggests that it would be difficult to accommodate a glutamic acid at position 185. The phosphorylase kinase

deficiency results support the notion of the crucial role in the correct conformation of the activation segment for substrate recognition.

Apolar contacts exist between the aliphatic portion of Arg(–3) and Phe112 from PHKγ_t, and between the side chain of Met(–1) and atoms of the glycine-rich loop. The most extensive apolar interaction, however, involves Phe(+1) which sits in a hydrophobic pocket formed from Val183, Pro187 and Leu190 from the enzyme, together with Leu(+3) from the peptide substrate (Figure 2B). The side chain of Leu(+3) itself interacts with this same apolar pocket, as well as with residue Met235′ from a crystallographic 2-fold related molecule. This interaction is one of the contacts defining a dimer formed within this crystal form, which also involves the carboxyl group of the peptide interacting with the peptide nitrogen of Met235′, and the peptide oxygen of Arg(+2) interacting with the peptide nitrogen of Lys234′.

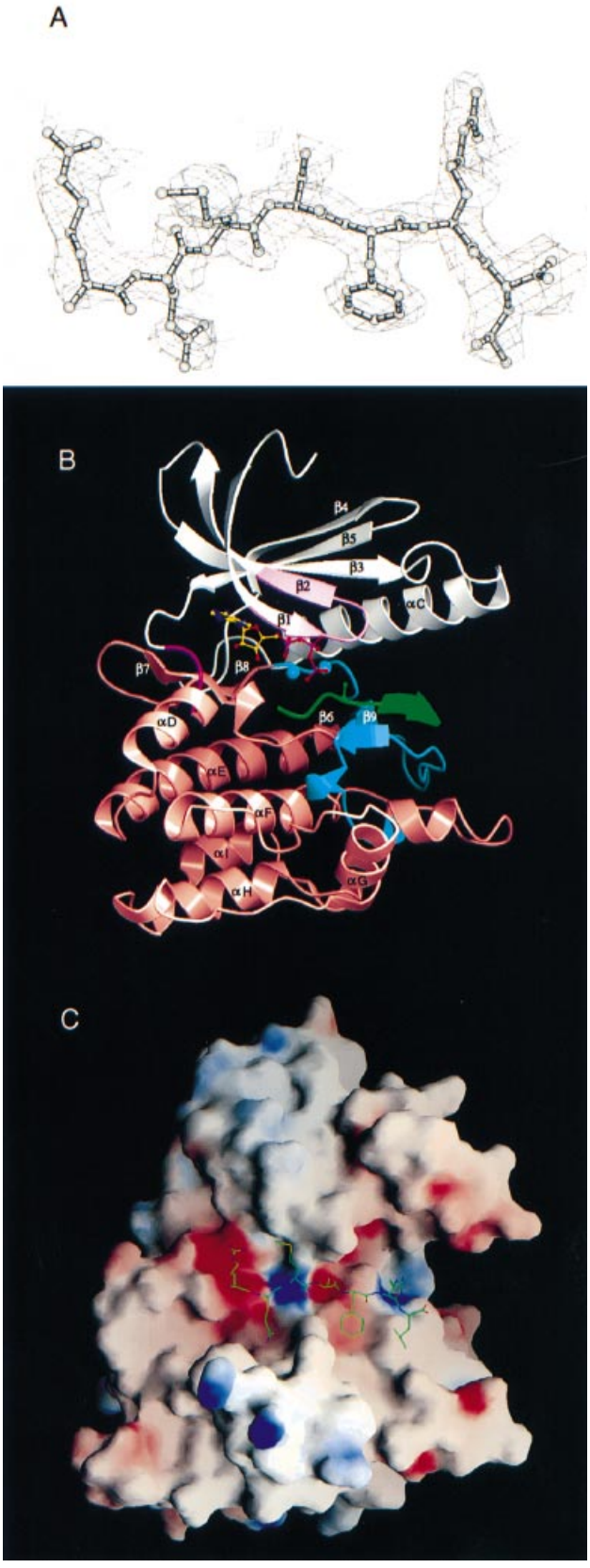

Fig. 1. Binding of the MC-peptide to PHKγ_t. (**A**) Electron density from the final refined $2F_o$–F_c map defining the conformation of the peptide. The map was calculated using $2mF_o$–DF_c coefficients output on the final cycle of REFMAC refinement, and is contoured at 0.2 $e^-/Å^3$ (= 0.9 σ), with contours further than 2.0 Å from peptide atoms deleted for clarity. (**B**) Location of the peptide-binding site with respect to the kinase catalytic domain. The PHKγ_t fold is shown with the N-terminal domain in white, the glycine-rich hairpin (residues 26–33) in pale magenta, the hinge region (residues 108 and109) in magenta, the C-terminal domain in salmon pink and the activation segment (residues 167–193) in cyan. AMPPNP is shown in individual atomic colours, with two manganese ions in cyan and the peptide shown in green, forming a short anti-parallel β-sheet with a part of the activation segment. (**C**) GRASP (Nicholls and Honig, 1991) representation of the surface to which peptide is bound. The molecular surface of PHKγ_t is coloured according to electrostatic potential such that deep blue corresponds to a potential of 30 kT, and deep red corresponds to a potential of –30 kT. The MC-peptide is shown as bonded atoms.

Comparison with other conformations of kinase-binding peptides

The conformation of the MC-peptide, closely related to the naturally occurring substrate of PHK, can be compared with the conformations of two other relevant peptides: firstly, with that of the tight binding inhibitor PKI in complex with cAPK (Bossmeyer *et al.*, 1993; Zheng *et al.*, 1993a), and secondly with the naturally occurring substrate of PHK in conformations which it adopts when not bound to PHK. These comparisons are presented in Figure 3.

As noted, the binding of the MC-peptide to PHKγ_t resembles closely the binding of PKI to cAPK. Both the conformation and the contacts of Arg(–3) are common to the two proteins. Gln(–2) differs from PKI, which has an arginine in the equivalent locus. Whereas the arginine of PKI interacts with Glu230 of cAPK, Gln(–2) of the MC-peptide interacts with Ser188. PHK has a threonine residue (Thr221) in place of Glu230 of cAPK. The conformation and contacts of Met(–1) resemble those of the equivalent glutamine residue of PKI, and the main chain conformation of Ser*(0) is close to that of the equivalent Ala in cAPK. Indeed, Ser*(0) of the MC-peptide can simply be constructed from Ala(0) of PKI by attachment of the OG atom with a $\chi1$ value of 61°. Phe(+1) is bound in a similar fashion to the equivalent isoleucine residue of PKI, but there is a significant difference in the conformation and contacts of Arg(+2) and Leu(+3) from those of the equivalent histidine and aspartate residues in PKI. Arg(+2) interacts with Glu182, the residue equivalent to the phosphorylated Thr197 of cAPK. This interaction site is not available to the histidine of PKI, since it is occupied by a histidine residue (His87) from the N-terminal domain

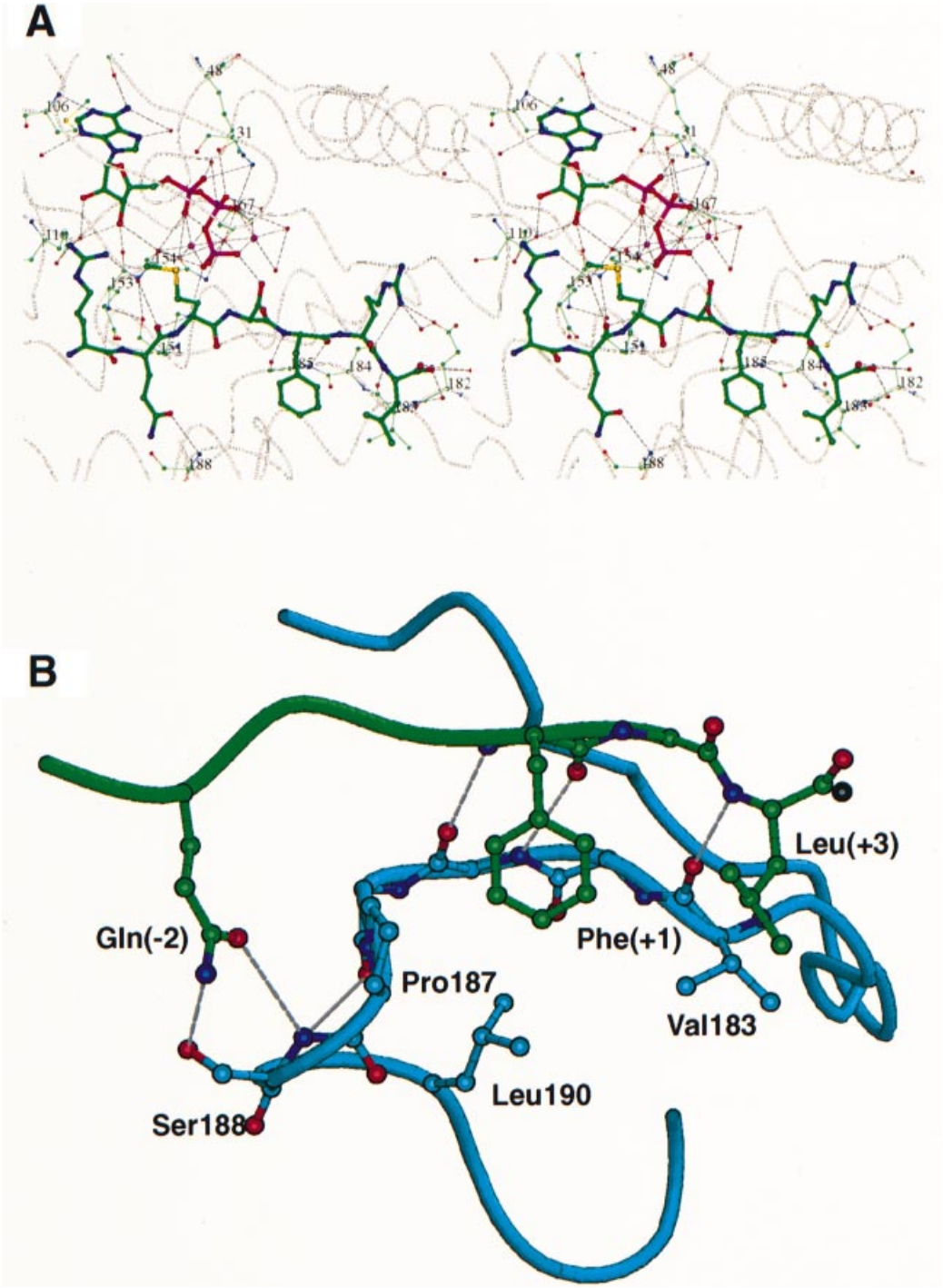

Fig. 2. Contacts of the MC-peptide to PHKγ_t. (**A**) (Stereo) Polar contacts (<3.4 Å) involved in binding nucleotide and peptide substrates to PHKγ_t are shown, with the residues involved labelled at their CA position. The backbone of the PHKγ_t molecule is shown as a faint worm representation, with atoms of protein residues shown as lines. Atoms of AMPPNP and the MC-peptide are shown in thicker ball and stick representation. Labelled residues from the protein are Ser31, Lys48, Met106, Glu110, Lys151, Glu153, Asn154, Asp167, Glu182, Val183, Cys184, Gly185 and Ser188. (**B**) Interactions of the MC-peptide with residues at the end of the activation segment. The MC-peptide is shown with green carbon atoms, while the activation segment is shown with cyan carbon atoms.

of cAPK. His(+2) of PKI, by contrast, is not involved in any direct polar interactions with the kinase. The conformation observed for the C-terminal two residues of the MC-peptide is necessary to allow the short stretch of anti-parallel β-sheet which exists between the substrate and the kinase activation loop in the complex described here, which is not apparent in the PKI–cAPK interaction (Figure 2B).

The conformations of residues 11–17 in GPa and GPb differ from each other (Barford *et al.*, 1991) and from the conformation of the MC-peptide in the ternary complex. In GPb, the N-terminal residues adopt an irregular conformation, with Ser14 and Val15 nearly α-helical. In GPa, the conformation around Ser14 is extended, although residues 15–17 have an α-helical conformation, which allows the Ser14 phosphate group to make hydrogen bonds

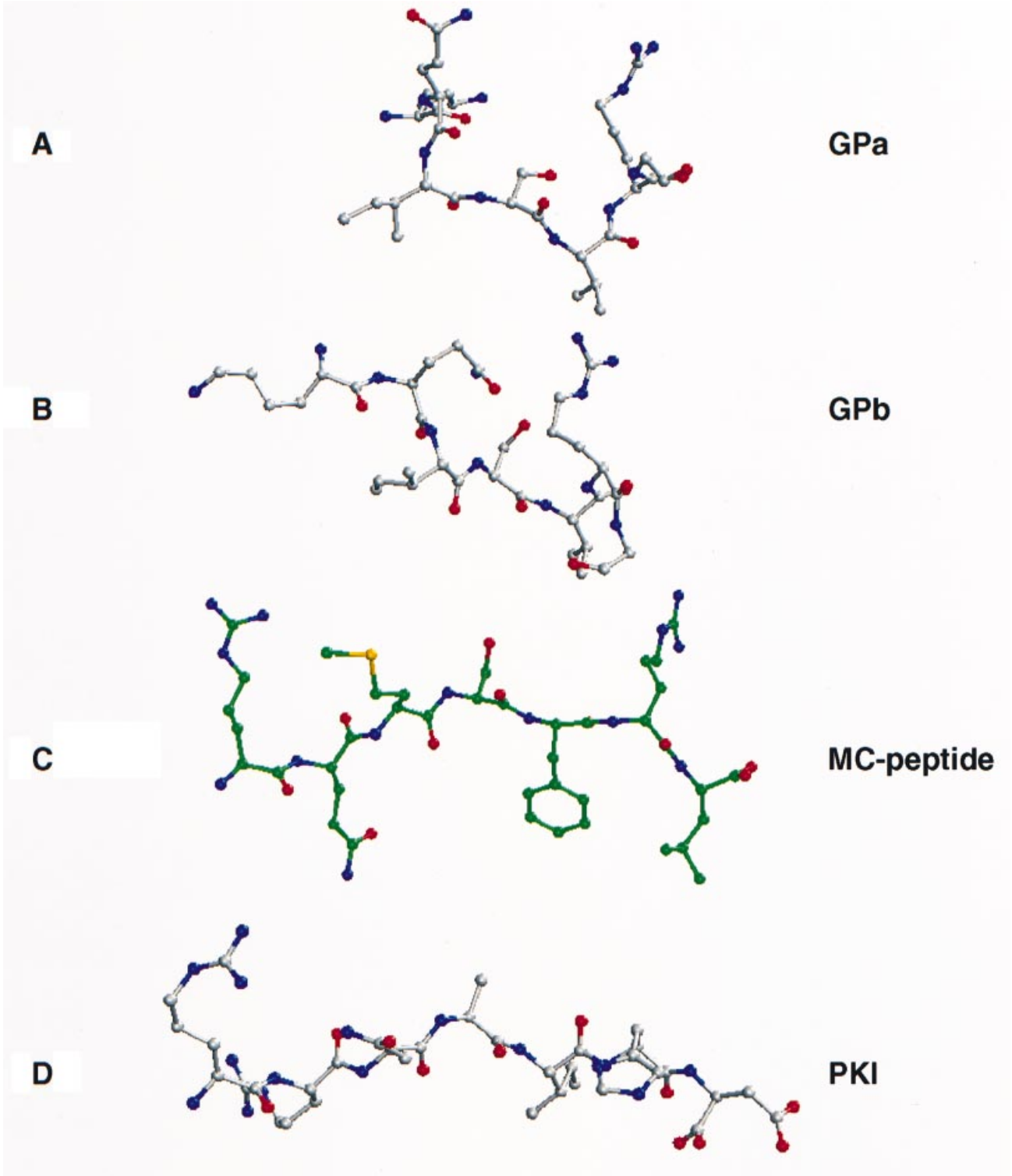

Fig. 3. Conformations of kinase inhibitor and substrate peptides. (**A**) Conformation of residues 11–17 of GPa. (**B**) Conformation of residues 11–17 of GPb. (**C**) Conformation of the MC-peptide, as observed in complex with PHKγ_t. (**D**) Conformation of the equivalent part of the protein kinase inhibitor peptide, as observed in complex with cAPK.

with the main chain nitrogens of residues 15 and 16. The conformation of the MC-peptide bound to PHKγ_t is all β. The N-terminal residues 11–19 in GPb exhibit high *B*-factors and are mobile. Mobility in the region around the site of phosphorylation appears to be essential to allow the substrate to be accommodated in the defined conformation when bound to the kinase, and may be a common feature of sites of phosphorylation in other proteins.

Dimerization

Although crystallized with only one molecule in the crystallographic asymmetric unit, two PHKγ_t molecules associate across a crystallographic 2-fold axis to form an

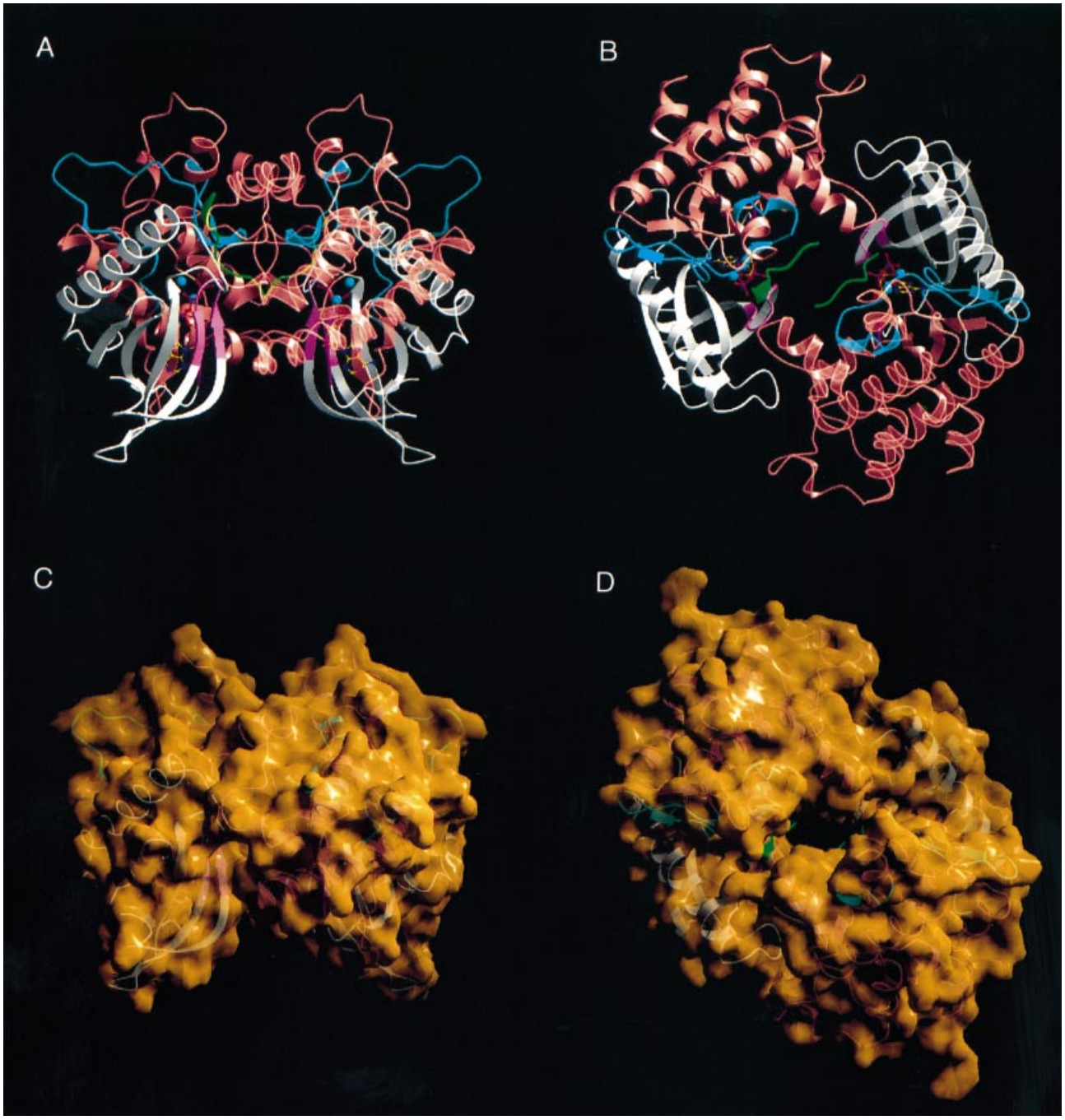

Fig. 4. Dimerization of PHKγ_t in this crystal form. Orthogonal views (**A**) perpendicular to the molecular 2-fold axis and (**B**) along the molecular 2-fold axis. Two crystallographically related PHKγ_t molecules are shown, coloured according to Figure 1B, with one molecule given partial transparency for distinction. (**C**) As (A), but with the molecular surface rendered. (**D**) As (B), but with the molecular surface rendered. Residues which undergo a change in accessible surface area upon dimerization (considering only changes caused by protein–protein contacts) are as follows: 24, 27, 29, 30, 54–59, 62, 65, 66, 69, 112, 113, 169, 170, 224–226, 230–233, 236, 247, 249, 250 and 252.

intimate dimer. Dimerization occurs in a head-to-tail fashion, such that residues at the N-terminus of the C-helix of each molecule interact with residues at the N-terminus of the G-helix of the other. Figure 4A and B shows this dimerization, with residues that undergo a change in surface area upon dimerization listed. The total change in accessible surface area due to dimerization is 2068 Å^2 (considering only kinase surface area), or 3160 Å^2 (considering protein + peptide surface area). The molecular surface formed by the resulting dimer is presented in Figure 4C and D. Interestingly, the MC-peptide is also involved in contacts across this 2-fold axis, with the contacts listed above from the last two residues of the MC-peptide to residues Lys234 and Met235 of the 2-fold related kinase molecule. These contacts involve the terminal leucine of the MC-peptide. In the natural substrate peptide, this residue is replaced by a glycine. It is possible that the lattice contacts mediated by the leucine contribute to the fact that crystals of the MC-peptide ternary complex, but not the natural substrate peptide ternary complex, have

been grown, although the interactions of Leu(+3) <4.0 Å in length involve its main chain atoms only.

The mode of dimerization does not correspond to the dimerization described for the fibroblast growth factor (FGF) receptor kinase (Mohammadi *et al.*, 1996), but does appear to bring the activation segment of each kinase monomer into relatively close apposition with the catalytic site of its partner, and for this reason may reflect the approach of two kinase molecules involved in transactivation (Figure 4B). The distance between the active sites of the two monomers is ~14 Å, which differs considerably from the GPb Ser14–Ca–Ser14′–Ca distance of 61.6 Å, but is closer to the GPa Ser14–Ca–Ser14′–Ca distance of 28.8 Å. PHK is active as a hexadecameric entity containing four copies of the catalytic γ-subunit arranged as a dimer of dimers (Norcum *et al.*, 1994), and acts upon a dimeric GPb substrate. This gives rise to the speculation that the dimerization observed in these crystals may reflect a functional state of PHK.

Comparison of protein, nucleotide conformation and metal ions in different ternary complexes

The conformations of the PHKγ_t ternary complex with the MC-peptide, and the cAPK ternary complex with PKI resemble each other very closely (Figure 5A). The only structural differences close to the active site involve the relative position of the glycine-rich nucleotide-binding hairpin, which is somewhat more open in the PHKγ_t complex as a result of a serine residue in place of the third glycine (Owen *et al.*, 1995a). At a more remote position, there is a marked difference in the orientation of the C- and G-helices of the two complexes. The C-helix is known to adopt a variety of positions in different kinase structures (e.g. Knighton *et al.*, 1991; De Bondt *et al.*, 1993; Jeffrey *et al.*, 1995; Sicheri *et al.*, 1997; Xu *et al.*, 1997). The structure presented here provides evidence that its orientation can also differ between two serine/threonine kinases in fully activated conformation.

One striking feature of the comparison between the PHKγ_t ternary complex with the MC-peptide and the cAPK ternary complex with PKI (Bossmeyer *et al.*, 1993; Zheng *et al.*, 1993a,b) is the extent of the similarity in conformation of the nucleotides and the coordination of the metal ions in the two kinase structures. Both manganese ions are coordinated in an octahedral fashion (Figure 2A). Mn1 is coordinated by terminal oxygens from the α- and γ-phosphates of AMPPNP, the bridging NH between the β- and γ-phosphates of AMPPNP, the amide oxygen of Asn154, a carboxyl oxygen from Asp167 and a water molecule. Mn2 is coordinated by terminal oxygens from the β- and γ-phosphates of AMPPNP, the two carboxyl oxygens of Asp167 and two water molecules. This conservation of co-factor conformation between two kinases sharing 33% sequence identity suggests a close conservation of mechanism.

Changes in protein conformation and flexibility

The ternary complex structure also shows that there is little change in conformation displayed by PHKγ_t upon peptide substrate binding. Superposition of the binary and ternary complexes (Figure 5B) shows a slight relative closure of the domains in the ternary complex, corresponding to a rotation of 3.4°. Other conformational differences occur only at the N-terminus of the C-helix (residues 56–61), in the region of the G-helix (residues 231–235 and 250–255) and at the C-terminal end of that part of the molecule which is well defined by electron density (residues 289–291). The first two of these regions correspond to residues involved in the dimerization described above, and it appears to be this, rather than a direct influence of substrate binding, that results in the structural alterations. The C-terminal residues 289–291 were noted in the binary complex to be more intimately associated with a crystallographically related molecule than with the kinase core domain itself, and this observation also applies in the ternary complex. Indeed, residues 292–298, which are part of the expressed protein, are not visible in the electron density maps of either structure.

Although little change is observed in the protein conformation, the binding of the MC-peptide, coupled with the formation of an intimate crystallographic dimer, has a marked effect on the apparent flexibility of the PHKγ_t molecule, as indicated by the temperature factor coloured plots in Figure 5C and D. The average main chain atomic temperature factor of PHKγ_t in the ternary complex is 28 Å^2, compared with 45Å^2 for the binary complex, with most of the difference concentrated at the regions described above to be involved in dimerization.

Implications for the catalytic mechanism

The most detailed studies on the catalytic mechanism have been performed with cAPK. Because of the similarities in the constellation of groups at the catalytic site, it is anticipated that PHK and cAPK should share similar catalytic properties. For cAPK, stereochemical arguments indicate that the γ-phosphate of ATP is transferred to the hydroxyl of serine by direct, nucleophilic displacement (Ho *et al.*, 1988). Kinetic studies indicate a random kinetic mechanism, although initial binding of ATP is preferred. Enzymatic phosphorylation proceeds with rapid equilibrium binding of substrates, and the chemical step is fast (500/s) relative to the rate-determining dissociation of the product ADP, when levels of Mg^{2+} and ATP are high (Adams and Taylor, 1992; Grant and Adams, 1996). Metal ions are needed not only for the fast transfer of the phosphate group but also for the rapid formation of a productive substrate complex (Adams and Taylor, 1993a). The effects of pH on phosphorylation of peptide substrates led to proposals for a general base-catalysed reaction (Yoon and Cook, 1987). Support for the assignment of Asp166 to this role has come from structural results which showed the proximity of Asp166 in cAPK to the substrate (Madhusudan *et al.*, 1994) and mutagenesis studies where, in the yeast enzyme, mutation of the corresponding residue to alanine led to an enzyme with 0.4% activity of the wild-type protein (Gibbs and Zoller, 1991). It is proposed that the general base accepts a proton from the seryl hydroxyl concurrent with nucleophilic attack of the alcoholate ion on the γ-phosphate of ATP. However, Adams and Taylor (1993b) have shown that the p*K*a value of 6.4 seen in pH rate studies is removed on alteration of the substrate but still allows efficient catalysis, which suggests that if the mechanism involves a general base, the ionization of this base is not manifested in the pH rate profiles. Grant and Adams have suggested that the hydrogen bond between Asp166 and the seryl substrate

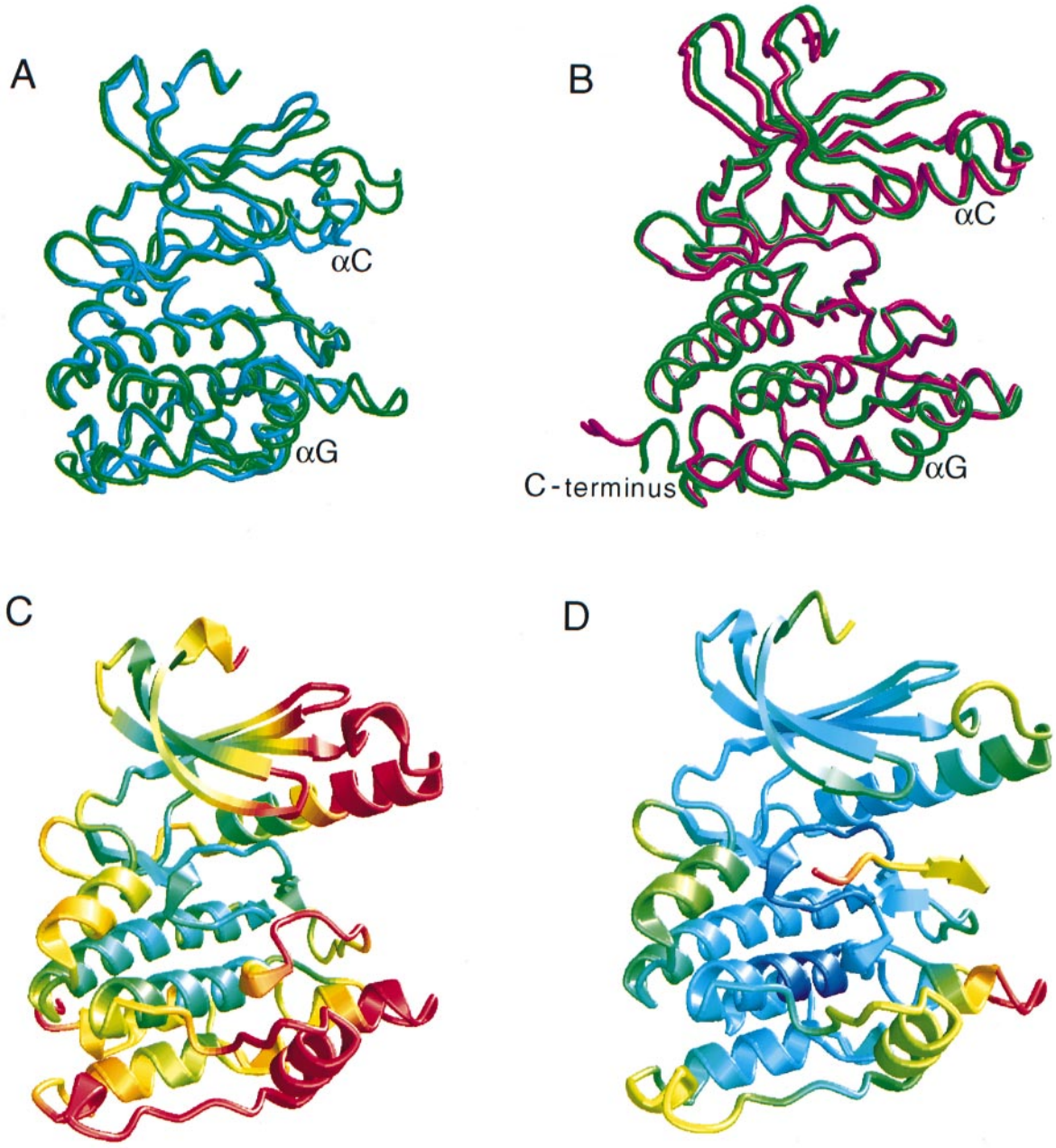

Fig. 5. Comparison of the PHKγ_t ternary complex protein conformation and flexibility with cAPK and the PHKγ_t binary complex. (**A**) Superposition of the catalytic cores of PHKγ_t ternary complex (green) and cAPK ternary complex (cyan). (**B**) Superposition of the PHKγ_t ternary complex (green) and the PHKγ_t binary complex (magenta). (**C**) Colour ramped fold of the PHKγ_t binary complex, such that blue corresponds to a CA atomic temperature factor of 10 Å^2 and red corresponds to a CA atomic temperature factor of 60 Å^2. (**D**) Colour ramped fold of the PHKγ_t ternary complex, such that blue corresponds to a CA atomic temperature factor of 10 Å^2 and red corresponds to a CA atomic temperature factor of 60 Å^2.

may not lower the ground state of the Michaelis complex but rather could isolate a productive rotamer for in-line transfer.

In PHKγ_t, the peptide substrate serine OG atom is 3.6 Å from the γ-phosphorus atom of the AMPPNP and is hydrogen bonded to one of the phosphate oxygens which in turn contacts the metal, Mn2 (Figure 6A). The conserved aspartate, equivalent to Asp166 in cAPK, is Asp149 in PHK. In the present structure, the aspartate OD2 atom is roughly equidistant from both the substrate Ser OG (4.3 Å) and the γ-phosphate oxygen (4.1 Å). These distances are large and would argue against a direct participation of the aspartate as a base. One interpretation of these observations is that the structure resembles a state in which the ATP could abstract the serine proton, after which a tighter interaction would result between ATP and the aspartate, which could share the abstracted proton. An alternative possibility is that the mechanism resembles more closely that proposed by Cole *et al.* (1995) in their work on Csk in which the aspartate acts to enhance the reactivity of the γ-phosphate of ATP to electrophilic attack. In this mechanism, deprotonation occurs after the phosphate ester bond is formed.

The complex in the crystal is with the inactive substrate analogue AMPPNP, which has a poor leaving group, and which may differ in ionization properties and possible

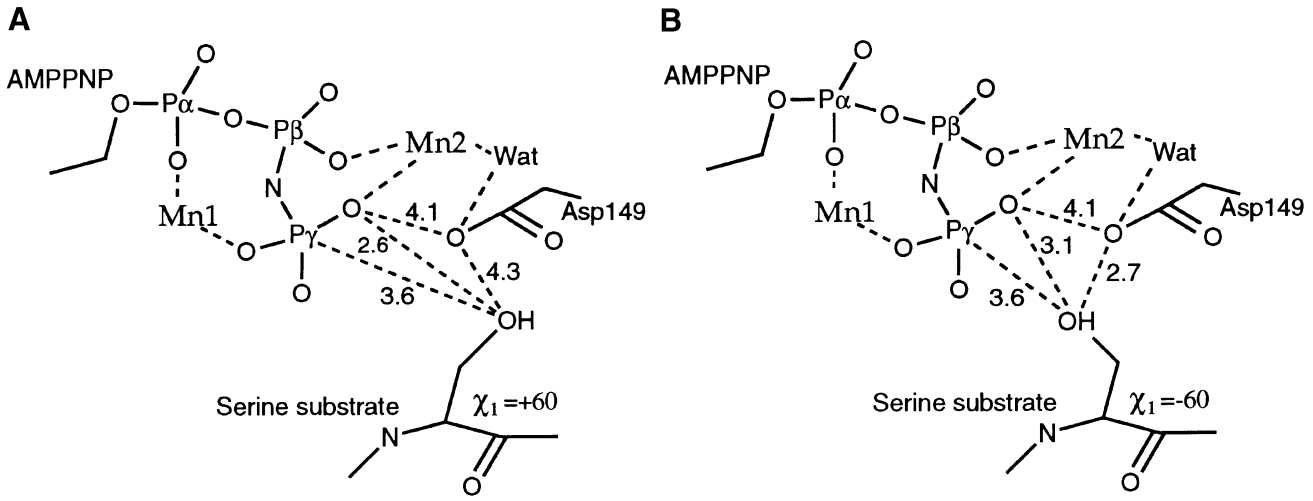

Fig. 6. Interactions of nucleophile, base and phosphate group. Interactions which might occur in a general base-catalysed reaction mechanism via: (**A**) the observed structure of the ternary complex and (**B**) an alternative conformation modelled by giving the attacking serine residue a χ1 angle of –60°.

conformation from the natural substrate ATP, although comparison of ATP and AMPPNP binding in cAPK showed minimal differences. It is possible that further conformational changes accompany catalytic turnover. Indeed, if the χ1 angle of the serine substrate is modified from +60°, as observed in the crystal structure, to the alternate rotamer –60°, then the OG atom is within 2.7 Å of the Asp149 OD2, 3.6 Å from the AMPPNP γ-phosphorus atom and 3.1 Å from the γ-phosphate oxygen (Figure 6B). This conformation would be consistent with a role for the aspartate as a base to promote attack on the ATP, but it is not yet supported by direct experimental evidence. In both rotamers, the OG atom is in line with the leaving group, although slightly better aligned in the latter position, to allow nucleophilic displacement. The triphosphate group is positioned by contacts to the metals and through contact to a lysine residue so that the negative charge developed during catalysis is both favoured and stabilized.

The ternary complex was obtained in the presence of Mn^{2+}. There are some differences in kinetic properties of PHKγ_t when assayed in the presence of Mg^{2+} or Mn^{2+}. The K_m values for ATP are similar while the K_m for GPb is 4-fold less in the present of Mn^{2+} (Yuan *et al.*, 1993). In the presence of Mg^{2+}, activity increases as magnesium concentration is increased to levels stoichiometric with ATP, and there is a further activatory effect with increased Mg^{2+} concentrations. In the presence of Mn^{2+}, activity increases up to Mn^{2+} concentrations stoichiometric with ATP, and higher concentrations of manganese inhibit (Kee and Graves, 1987; Cox and Johnson, 1992). Comparison of Mg^{2+} and Mn^{2+} ion positions in complexes with both cAPK and PHKγ_t showed no significant differences (Zheng *et al.*, 1993b; Owen *et al.*, 1995a), and examination of the PHKγ_t structure showed no other metal-binding sites. It is assumed that the different effects on the kinetics must be mediated through the observed crystallographic binding sites which are identical for Mg^{2+} and Mn^{2+}. There are no direct interactions of the peptide substrate with the metal ions, although the seryl hydroxyl could make a long (3.6 Å) hydrogen bond to one of the Mn2 water-bound molecules. Studies with cAPK have shown that the site Mn2, which bridges the β- and γ-phosphates, is the high affinity (activatory) site (Zheng *et al.*, 1993a). In cAPK, the rate-limiting step in the reaction is release of ADP product. By inference with PHKγ_t, we may expect the second metal site, Mn1, which bridges the α and γ sites in the AMPPNP complex and the α and β sites in the ADP complex, to play a significant role in the inhibitory mechanism of Mn^{2+}. It may be that in PHKγ_t, occupation of the Mn1 site by Mg^{2+} favours formation of product through neutralization of the developing negative charge, while the occupation of this site by Mn^{2+}, although it may also favour formation of product, might inhibit release of product more severely. At pH 8.0, the dissociation constants of the two metals for ATP are similar (13.7 μM for Mg^{2+} and 10 μM for Mn^{2+}) but there is almost a 10-fold difference in the dissociation constants for ADP (250 μM for Mg^{2+}; 33 μM for Mn^{2+}) (O'Sullivan and Smithers, 1979). An explanation for the kinetic effects could be provided if such tighter binding were also manifested in the association of MnADP to the kinase, but this remains to be tested.

Discussion

The relative Michaelis–Menten parameters of the natural substrate peptide and the modified Cantley peptide correlate well with those expected on the basis of the site by site preference values determined by Songyang *et al.* (1996) (see Table I). Two reasons may explain why the approach of Songyang *et al.* can identify peptide substrates with superior kinetic parameters to peptides from the natural substrate. Firstly, the fact that, in a protein kinase system, catalytic parameters are tuned to regulate the activity of the substrate, rather than to maximize turnover. Secondly, the fact that peptide recognition is only a part of the substrate binding event, with the rest constituted by kinase–substrate interactions remote from the phosphorylatable residue. Both peptide substrates have a K_m ~50-fold higher than that of intact phosphorylase as a

substrate, suggesting that significant binding affinity derives from remote interactions between PHK and GPb.

The structure of the ternary complex of PHKγ_t with AMPPNP and the MC-peptide allows rationalization of the subsite determinants of the substrate specificity of PHK. Complementary side chain interactions for the positive charges at Arg(–3) and Arg(+2) and for the hydrophobic residue Phe(+1) would be anticipated to govern the binding of a peptide to the PHK catalytic core. Unexpected from the PKI–cAPK complex is the existence of a short β-sheet formed between the PHKγ_t activation segment and the MC-peptide substrate. Main chain interactions of Phe(+1) and Leu(+3) in this β-sheet dictate the position of the main chain of the phosphorylatable residue Ser(0). Since the position of the terminal OG of Ser(0) is fixed relative to the γ-phosphate of ATP, a preferred length of the side chain of the phosphorylatable residue is defined. This defined length may explain the selectivity of PHK for serine/threonine over tyrosine. No activity of PHKγ_t against a peptide equivalent to the MC-peptide, but with a tyrosine rather than a serine in the phosphorylatable position, was detected in the presence of either Mg^{2+} or Mn^{2+} (data not shown), although a measurable activity has been reported for PHK against angiotensin in the presence of Mn^{2+} (Yuan *et al.*, 1993).

The β-partner of the short substrate β-strand is formed from residues 183–185 of the activation segment. Further interactions occur between the side chain of Gln(–2) and residue Ser188, and between Phe(+1) and residues Val183, Pro187 and Leu190, all of which lie in the activation segment (Figure 2B). The role of the activation segment in determining the relative orientation of the N- and C-terminal domains, and in modulating details of active site geometry have been noted previously (Johnson *et al.*, 1996). The observation here of extensive interactions between the activation segment and a peptide substrate identifies another mechanism by which the detailed conformation of this segment can influence kinase activity. This further explains why residues of the activation segment are so frequently responsible for control by reversible phosphorylation.

The high degree of structural similarity that exists between the AMPPNP–MC-peptide–PHKγ_t ternary complex and the AMPPNP–PKI–cAPK ternary complex probably identifies the details of conformation which represent a serine/threonine kinase poised for catalytic turnover. It is interesting then to note that these ternary complexes differ from the phosphorylated complex of CDK2 with cyclin A (Russo *et al.*, 1996) in several details of active site structure and nucleotide conformation (data not shown). This suggests that there may be a further subtle change in CDK2 conformation in forming the productive ternary complex. In this case, CDK2 would differ from PHK, which shows little change between nucleotide binary complex and nucleotide–peptide ternary complexes.

The existence of a dimer in the crystals of the ternary complex raises the possibility that a similar dimer may be involved in activity upon the dimeric GPb substrate. This possibility is consistent with the existence of the catalytic domain of PHK in a complex oligomeric structure. Immunolabelling experiments have mapped the non-catalytic α-subunit of PHK to the tips of the hexadecameric holoenzyme (Wilkinson *et al.*, 1994), and an epitope consisting of residues 277–290 of the γ-subunit to a site on the interior lobe face of the holoenzyme, remote from any of the 2-fold axes of the molecule (Wilkinson *et al.*, 1997). The location of the γ-subunit at a position remote from the 2-fold axes of the assembly is not obviously consistent with the dimer observed here being present in the holoenzyme. It should be noted, however, that the epitope 277–290 falls on the 'back' of the kinase catalytic domain, 32 Å away from the dimerization 2-fold axis discussed here. Although we have been unable to isolate a dimeric ternary complex in solution by gel filtration, it remains a tantalizing possibility. The existence of a dimeric kinase subunit would provide a cooperative explanation for the significantly higher affinity of PHK for intact dimeric phosphorylase over the equivalent monomeric sequence as a peptide.

Materials and methods

Protein production

PHKγ_t, comprising residues 1–298 of the rabbit muscle PHK γ-subunit, was prepared by the method previously described (Owen *et al.*, 1995b). PHKγ_t was refolded from inclusion bodies and purified using anion exchange chromatography followed by affinity chromatography on Cibachron blue. Crystallizations were carried out on the day following the final purification step. GPb was isolated from rabbit skeletal muscle as previously described (Melpidou and Oikonomakos, 1983). Peptides were synthesized on an Applied Biosystems 430A Automated Peptide Synthesizer, using standard Fmoc methodology.

Phosphorylation assays

The phosphorylation of peptide substrates was measured spectrophotometrically using an assay which couples the phosphorylation event with the oxidation of NADH (Cook *et al.*, 1982; Adams *et al.*, 1995). All reactions were carried out at 30°C in a total volume of 0.3 ml. The assay mixture contained buffer [50 mM Tris, 50 mM HEPES, 0.5 mM calcium chloride, 2 mM dithiothreitol (DTT), 10 mM magnesium acetate, pH 8.2] and 0.1 mg/ml bovine serum albumin (BSA), 3.6 U of lactate dehydrogenase, 1.2 U of pyruvate kinase, 1 mM phosphoenolpyruvate and 0.2 mM NADH. The peptide concentration was varied from 0.1 to 2 mM. The reaction was initiated by the simultaneous addition of PHKγ_t to 0.5 μg/ml and ATP to 1 mM. The phosphorylation of GPb by PHKγ_t was determined using two methods which gave similar results. The first was the phosphocellulose radioisotopic assay (Roskoski, 1983). Reactions were carried out at pH 8.2 using varying concentrations of GPb and [γ-^{32}P]ATP (100 c.p.m./pmol) (0.8–7 mg/ml and 0.04–1 mM respectively) and the reaction was initiated by the addition of PHKγ_t to 50 ng/ml. Conversion of GPb to GPa was also monitored by assaying phosphorylase activity in the presence of 10 μM AMP and 0.5 mM caffeine in the direction of glycogen synthesis. Varying concentrations of GPb (1–10 mg/ml) and ATP (0.04–1.5 mM) were used, and peptide, when present, was used at 1 mM. Inorganic phosphate released in the phosphorylase reaction was determined and initial reaction rates calculated from the pseudo-first order reaction constants as described (Oikonomakos *et al.*, 1995). Kinetic data were analysed by the use of the non-linear regression program GRAFIT (Leatherbarrow, 1992).

Higher resolution binary complex

Following the previous description of the structure of a PHKγ_t–AMPPNP binary complex (Owen *et al.*, 1995a), an additional data set to 2.1 Å was recorded at the ESRF, Grenoble on beamline 4, using an X-ray image intensifier charge couple device detector (XRIICCD). Crystal growth and cryo-protection conditions were as in Owen *et al.* (1995b). Data were collected over a total range of 180°, in oscillations of 1° exposed for either 15 or 20 s. Images were corrected for spatial distortion and dark current by the program FIT2D, and subsequently processed using MOSFLM (Leslie, 1992) and programs of the CCP4 package (CCP4, 1994). Statistics of the dataset are given in Table II. Refinement of the structure was begun using the 2.5 Å structure described in Owen *et al.* (1995a) and pursued using alternating cycles of manual rebuilding in O (Jones *et al.*, 1991) and crystallographic minimization using XPLOR (Brunger, 1992).

Ternary complex

Crystallization. The ternary complex was crystallized using the hanging drop method of vapour diffusion from drops containing 1 µl of protein solution [2–3 mg/ml PHKγ_t, 10 mM MC-peptide, 3 mM AMPPNP, 10 mM HEPES/NaOH (pH 8.2), 2% (v/v) glycerol, 10 mM DTT, 0.2% w/v NaN_3, 0.1 mM EDTA, 5 mM $MnCl_2$] and 1 µl of reservoir solution [5% PEG 8000, 50 mM HEPES (pH 6.9), 10% (v/v) glycerol, 10 mM DTT, 0.02% w/v NaN_3 and 5 mM $MnCl_2$] at a temperature of 14°C. Crystals were first observed ~48 h after setting up the drops and continued to grow for 2–3 days. Crystals were harvested into a solution containing 12.5% PEG 8000, 10 mM MC-peptide, 5 mM $MnCl_2$, 50 mM HEPES/NaOH (pH 6.9), 10 mM DTT, 10% (v/v) glycerol.

X-ray data collection. Data for the ternary complex with the MC-peptide were collected using cryo-crystallography at 100 K (Teng, 1990). Crystals were transferred into a cryo-protectant buffer [12.5% PEG 8000, 10 mM MC-peptide, 5 mM $MnCl_2$, 50 mM HEPES/NaOH (pH 6.9), 10 mM DTT, 30% (v/v) glycerol] for a few seconds, prior to mounting in a 0.2 mm diameter nylon fibre loop (Hampton Research) in a gaseous nitrogen stream at 100 K generated by an Oxford Cryostream.

Initial X-ray diffraction data to 3.6 Å were collected from a single crystal with dimensions of ~200 µm×20 µm×20 µm on the Super ESCA beamline at ELETTRA, Trieste, using a 30 cm diameter Mar research image plate in 18 cm mode. The synchrotron was operated at a wavelength of 0.90 Å. Data were collected using 1.5° oscillations exposed for 240 s, over a total rotation of 42.5°. The crystals were trigonal space group $P3_221$ with unit cell dimensions $a = b = 64.1$ Å, $c = 144.4$ Å. Data were processed using DENZO and its companion program SCALEPACK (Otwinowski, 1993).

Following the growth of larger crystals, X-ray diffraction data were collected to 2.6 Å from a single crystal with dimensions ~400 µm× 30 µm×30 µm on station D2AM at the ESRF, Grenoble, using an XRIICCD detector. The synchrotron was operated at a wavelength of 0.90 Å. Data were collected using 0.3° oscillations, exposed for 60 s, over a total rotation of 33.6°. The crystals were trigonal space group $P3_221$ with unit cell dimensions $a = b = 65.3$ Å, $c = 145.8$ Å. Data were corrected for spatial distortion by the program CCDTOIP (M.E.M.Noble, unpublished work), and processed further by the program MOSFLM (Leslie, 1992), followed by data reduction using programs of the CCP4 suite (CCP4, 1994). Statistics for both of these data sets are given in Table II.

Structure solution. The structure was initially solved for the 3.6 Å data set by molecular replacement using the 2.1 Å binary complex structure as a search model in the program AMoRe (Navaza, 1990). The translation function confirmed the space group as $P3_221$, giving a correlation coefficient of 60.0% and a crystallographic *R*-factor of 39.6%, compared with the next highest solution which had a correlation coefficient of 33.3%. An electron density map, based upon phases from the molecular replacement solution, immediately showed the position of the entire peptide backbone of both the protein and its complexed peptide substrate with the positions of most side chains being apparent. Model building and refinement were carried out using alternating cycles of manual refitting in O, and initial rigid-body refinement in X-PLOR followed by further refinement in REFMAC (Murshudov *et al.*, 1997), until a free *R*-value of 35.3% was achieved. At this point, the higher resolution dataset was obtained and further refinement was continued against these data. Water molecules were added to the model at positions showing large positive peaks in F_o–F_c electron density, where the resultant water molecule would be in a favourable hydrogen bonding environment.

Acknowledgements

The authors would like to acknowledge the help of Maureen Pitkeathly from the Oxford Centre for Molecular Sciences Peptide Synthesis Unit, and Elspeth Garman for her help in the search for soaking conditions to bind peptides to the orthorhombic form of PHKγ_t crystals. We would also like to thank Dr A.Mamalaki and Dr S.J.Tzartos of the Hellenic Pasteur Institute, Department of Biochemistry, for help in the expression of PHKγ_t, and H.Gika and C.Kravariti for work in the kinetic experiments. At synchrotron beam lines, we would like to thank Dr Luca Olivi (Elletra), Dr Andrew Hammersley (XRIICCD experiment on ESRF BL4) and Dr Richard Kahn (D2AM, ESRF). Support at the Laboratory of Molecular Biophysics by Dr Richard Bryan and Dr Kathryn Measures (computing), and Steve Lee (photographic) is gratefully acknowledged. This work was supported in part by grants from the MRC (program grant to L.N.J.) and the Royal Society (University Research Fellowship to M.E.M.N.). The OCMS is funded jointly by the BBSRC and the MRC.

References

Adams,J.A. and Taylor,S.S. (1992) Energetic limits of phosphotransfer in the catalytic subunit of cAMP-dependent protein kinase as measured by viscosity experiments. *Biochemistry*, **31**, 8516–8522.

Adams,J.A. and Taylor,S.S. (1993a) Divalent metal ions influence catalysis and active site accessibility in the cAMP-dependent protein kinase. *Protein Sci.*, **2**, 2177–2186.

Adams,J.A. and Taylor,S.S. (1993b) Phosphorylation of peptide substrates for the catalytic subunit of cAMP-dependent protein kinase. *J. Biol. Chem.*, **268**, 7747–7752.

Adams,J.A., McGlone,M.L., Gibson,R. and Taylor,S.S. (1995) Phosphorylation modulates catalytic function and regulation in the cAMP-dependent protein kinase. *Biochemistry*, **34**, 2447–2454.

Barford,D., Hu,S.-H. and Johnson,L.N. (1991) The structural mechanism for glycogen phosphorylase control by phosphorylation and by AMP. *J. Mol. Biol.*, **218**, 233–260.

Bossmeyer,D., Engh,R.A., Kinzel,V., Ponstingl,H. and Huber,R. (1993) Phosphotransferase and substrate binding mechanism of the cAMP dependent protein kinase subunit from porcine heart as deduced from the 2.0 Å structure of the complex with Mn^{2+} adenylylimidophosphate and inhibitor peptide PKI(5–24). *EMBO J.*, **12**, 849–859.

Brunger,A.T. (1992) *X-PLOR: Version 3.1; A System for Protein Crystallography and NMR*. Yale University Press, New Haven, CT.

CCP4 (1994) The CCP4 (Collaborative Computational Project Number 4) suite: programmes for protein crystallography. *Acta Crystallogr.*, **D50**, 760–763.

Cole,P.A., Grace,M.R., Phillips,R.S., Burn,P. and Walsh,C.T. (1995) The role of the catalytic base in the protein tyrosine kinase Csk. *J. Biol. Chem.*, **270**, 22105–22108.

Cook,F.N., Neville,M.E., Vrana,K.E., Hartl,F.T. and Roskowski,R. (1982) Adenosine cyclic 3′,5′-monophosphate dependent protein kinase: kinetic mechanism for the bovine skeletal muscle catalytic subunit. *Biochemistry*, **21**, 5794–5799.

Cox,S. and Johnson,L.N. (1992) Expression of the phosphorylase kinase γ subunit catalytic domain in *E. coli*. *Protein Eng.*, **5**, 811–819.

De Bondt,H.L., Rosenblatt,J., Jancarik,J., Jones,H.D., Morgan,D.O. and Kim,S.-H. (1993) Crystal structure of cyclin dependent kinase 2. *Nature*, **363**, 592–602.

Gibbs,C.S. and Zoller,M.J. (1991) Rational scanning mutagenesis of a protein kinase identifies functional regions involved in catalysis and substrate interactions. *J. Biol. Chem.*, **266**, 8923–8931.

Grant,B.D. and Adams,J.A. (1996) Pre-steady state kinetic analysis of cAMP-dependent protein kinase rapid quench flow techniques. *Biochemistry*, **35**, 2022–2029.

Graves,D.J. (1983) Use of peptide substrates to study the specificity of phosphorylase kinase phosphorylation. *Methods Enzymol.*, **99**, 268–278.

Hanks,S.K. and Quinn,A.M. (1991) Protein kinase catalytic domain sequence database: identification of conserved features of primary structure and classification of family members. *Methods Enzymol.*, **200**, 38–62.

Ho,M.F., Bramson,H.N., Hansen,D.E., Knowles,J.R. and Kaiser,E.T. (1988) Stereochemical course of the phospho group transfer catalysed by cAMP-dependent prtoein kinase. *J. Am. Chem. Soc.*, **110**, 2680–2681.

Huang,C.-Y.F., Yuan,C.-Y., Blumenthal,D.K. and Graves,D.J. (1995) Identification of the substrate and pseudosubstrate binding sites of phosphorylase kinase γ subunit. *J. Biol. Chem.*, **270**, 7183–7188.

Jeffrey,P.D., Russo,A.A., Polyak,K., Gibbs,E., Hurwitz,J., Massague,J. and Pavletich,N.P. (1995) Mechanism of CDK activation revealed by the structure of a cyclinA–CDK2 complex. *Nature*, **376**, 313–320.

Johnson,L.N., Noble,M.E.M. and Owen,D.J. (1996) Active and inactive protein kinases. *Cell*, **85**, 149–158.

Jones,T.A., Zou,J.-Y., Cowan,S.W. and Kjeldgaard,M. (1991) Improved methods for building protein models in electron density maps and location of errors in these models. *Acta Crystallogr.*, **A47**, 110–119.

Kee,S.M. and Graves,D.J. (1987) Properties of the γ subunit of phosphorylase kinase. *J. Biol. Chem.*, **262**, 9448–9453.

Knighton,D.R., Zheng,J., Ten Eyck,L.F., Ashford,V.A., Xuong,N.-H., Taylor,S.S. and Sowadski,J.M. (1991) Crystal structure of the catalytic subunit of cyclic adenosinemonophosphate-dependent protein kinase. *Science*, **253**, 407–413.

Laskowski,R.A., MacArthur,M.W., Moss,D.S. and Thorton,J.M. (1993) PROCHECK: a programme to check the stereochemical quality of protein structures. *J. Appl. Crystallogr.*, **26**, 283–291.

Leatherbarrow,R.J. (1992) *GrafFit Version 3.0*. Erithakus Software, Staines, UK.

Leslie,A.G.W. (1992) *MOSFLM*. Daresbury Laboratory, Warrington, Vol. 26.

Madhusudan, Trafny,E.F., Xuong,N., Adams,J.A., Eyck,L.F.T., Taylor, S.S. and Sowadski,J.M. (1994) cAMP-dependent protein kinase: crystallographic insights into substrate recognition and phosphotransfer. *Protein Sci.*, **3**, 176–187.

Maichele,A.J., Burwinkel,B., Maire,I., Sovik,O. and Kilimann,M.W. (1996) Mutations in the testis/liver isoform of the phosphorylase kinase γ subunit cause autosomal liver glucogenosis in the gsd rat and in humans. *Nature Genet.*, **14**, 337–340.

Melpidou,A.E. and Oikonomakos,N.G. (1983) The effects of glucose-6-phosphate on the catalytic and structural properties of glycogen phosphorylase a. *FEBS Lett.*, **154**, 105–110.

Mohammadi,M., Schlessinger,J. and Hubbard,S. (1996) Structure of the FGF receptor tyrosine kinase domain reveals a novel autoinhibitory mechanism. *Cell*, **86**, 577–587.

Murshudov,G.N., Vagen,A.A. and Dodson,E.J. (1997) Refinement of macromolecular structures by the maximum-likelihood method. *Acta Crystallogr.*, **D53**, 240–255.

Navaza,J. (1990) AMoRe: an automated package for molecular replacement. *Acta Crystallogr.*, **A50**, 157–163.

Nicholls,A. and Honig,B. (1991) A rapid finite difference algorithm, utilising successive over relaxation to solve the Poisson Boltzmann equation. *J. Comput. Chem.*, **12**, 435–445.

Norcum,M.T., Wilkinson,D.A., Carlson,M.C., Hainfield,J.F. and Carlson,G.M. (1994) Structure of phosphorylase kinase. A three dimensional model derived from stained and unstained electron micrographs. *J. Mol. Biol.*, **241**, 94–102.

Oikonomakos,N.G., Zographos,S.E., Johnson,L.N., Papageorgiou,A.C. and Acharya,K.R. (1995) The binding of 2-deoxy-D-glucose-6-phosphate to glycogen phosphorylase b: kinetic and crystallographic studies. *J. Mol. Biol.*, **254**, 900–917.

O'Sullivan,W.J. and Smithers,G.W. (1979) Stability constants for biologically important metal–ligand complexes. *Methods Enzymol.*, **63**, 294–336.

Otwinowski,Z. (1993) DENZO. In Sawyer,L., Isaacs,N. and Bailey,S. (eds), *Data Collection and Processing*. SERC Laboratory, Daresbury, Warrington, UK, DL/SC1/R34, pp. 56–62.

Owen,D.J., Noble,M.E., Garman,E.F., Papageorgiou,A.C. and Johnson,L.N. (1995a) Two structures of the catalytic domain of phosphorylase kinase: an active protein kinase complexed with substrate analogue and product. *Structure*, **3**, 467–482.

Owen,D.J., Papageorgiou,A.C., Garman,E.F., Noble,M.E.M. and Johnson,L.N. (1995b) Expression, purification and crystallisation of phosphorylase kinase catalytic domain. *J. Mol. Biol.*, **246**, 376–383.

Paudel,H.K. (1997) The regulatory Ser^{262} of microtubule-associated protein tau is phosphorylated by phosphorylase kinase. *J. Biol. Chem.*, **272**, 1777–1785.

Paudel,H.K., Zwiers,H. and Wang,J.H. (1993) Phosphorylase kinase phosphorylates the calmodulin-binding regulatory regions of neuronal tissue-specific proteins B-50 (GAP-43) and neurogranin. *J. Biol. Chem.*, **268**, 6207–6213.

Pearson,R.B. and Kemp,B.E. (1991) Protein kinase phosphorylation site sequences and consensus specificity motifs. *Methods Enzymol.*, **200**, 62–81.

Pickett-Gies,C.A. and Walsh,D.A. (1986) Glycogen Phosphorylase Kinase. In Boyer,P.D. and Krebs,E.G. (eds), *The Enzymes.* Academic Press, Orlando, FL, Vol. 17, pp. 396–459.

Roskoski,R. (1983) Assays of protein kinase. *Methods Enzymol.*, **99**, 3–6.

Russo,A., Jeffrey,P.D. and Pavletich,N.P. (1996) Structural basis of cyclin dependent kinase activation by phosphorylation. *Nature Struct. Biol.*, **3**, 696–700.

Sicheri,F., Moarefi,I. and Kuriyan,J. (1997) Crystal structure of the Src family tyrosine kinase Hck. *Nature*, **385**, 602–609.

Songyang,Z. *et al*. (1996) A structural basis for substrate specificities of protein Ser/Thr kinases. *Mol. Cell. Biol.*, **16**, 6486–6493.

Teng,T.-Y. (1990) Mounting of crystals for macromolecular crystallography in a free standing thin film. *J. Appl. Crystallogr.*, **23**, 387–391.

Wilkinson,D.A., Marion,T.N., Tilman,D.M., Norcum,M.T., Hainfield,J.F., Seyer,J.M. and Carlson,G.M. (1994) An epitope proximal to the carboxyl terminus of the γ-subunit is located near the lobe tips of the phosphorylase kinase hexadecamer. *J. Mol. Biol.*, **235**, 974–982.

Wilkinson,D.A., Norcum,M.T., Fitzgerald,T.J., Marion,A.N., Tillma, D.M. and Carlson,G.M. (1997) Proximal regions of the catalytic γ and regulatory β subunits on the interior lobe face of phosphorylase kinase are structurally coupled to each other and enzyme activation. *J. Mol. Biol.*, **265**, 219–239.

Xu,W., Harrison,S.C. and Eck,M.J. (1997) Three dimensional structure of the tyrosine kinase c-Src. *Nature*, **385**, 595–602.

Yoon,M.-Y. and Cook,P.F. (1987) Chemical mechanism of the adenosine cyclic 3′,5′-monophosphate dependent protein kinase from pH studies. *Biochemistry*, **26**, 4118–4125.

Yuan,C.J., Huang,C.Y. and Graves,D.J. (1993) Phosphorylase kinase, a metal ion-dependent dual specificity kinase. *J. Biol. Chem.*, **268**, 17683–17686.

Zheng,J., Knighton,D.R., Eyck,L.F.T., Karlsson,R., Xuong,N., Taylor, S.S. and Sowadski,J.M. (1993a) Crystal structure of the catalytic subunit of cAMP-dependent protein kinase complexed with MgATP and peptide inhibitor. *Biochemistry*, **32**, 2154–2161.

Zheng,J., Trafny,E.A., Knighton,D.R., Xuong,N., Taylor,S.S., Eyck, L.F.T. and Sowadski,J.M. (1993b) 2.2 Å refined crystal structure of the catalytic subunit of cAMP-dependent protein kinase complexed with MnATP and a peptide inhibitor. *Acta Crystallogr.*, **D49**, 362–365.

Received on August 1, 1997; revised on September 5, 1997